PCCP

Threshold for Shattering Fragmentation in Collision-Induced Dissociation of the Doubly Protonated Tripeptide TIK$(H^+)_2$

Journal:	*Physical Chemistry Chemical Physics*
Manuscript ID	CP-COM-04-2018-002577.R2
Article Type:	Communication
Date Submitted by the Author:	12-Jul-2018

Complete List of Authors:	Macaluso, Veronica; CNRS - Université d\'Evry-Val-d\'Essonne, LAMBE UMR 8587 Homayoon, Zahra; Texas Tech University, Department of Chemistry and Biochemist Spezia, Riccardo; CNRS - Sorbonne Université, Laboratoire de Chimie Théorique UMR 7616; CNRS - Université d'Evry-Val-d'Essonne, LAMBE UMR 8587 Hase, William; Texas Tech University, Depart of Chemistry and Biochemistry

Threshold for Shattering Fragmentation in Collision-Induced Dissociation of the Doubly Protonated Tripeptide TIK$(H^+)_2$

Veronica Macaluso,[a] Zahra Homayoon,[b]
Riccardo Spezia[a,c,*] and William L. Hase,[b,*]

[a]LAMBE, Univ Evry, CNRS, CEA, Université Paris-Saclay, 91025 Evry (France)

[b]Department of Chemistry and Biochemistry
Texas Tech University
Lubbock, Texas 79409-1061 USA

[c]Sorbonne Université, CNRS, Laboratoire de Chimie Théorique, LCT, 4 Place Jussieu, 75252 Paris Cedex 05 (France)

* Correspondence to: riccardo.spezia@sorbonne-universite.fr and bill.hase@ttu.edu

Abstract

In a recent direct dynamics simulations of the collision induced dissociation (CID) of the doubly protonated tripeptide threonine−isoleucine−lysine and threonine−leucine−lysine ions, $TIK(H^+)_2$ and $TLK(H^+)_2$, a shattering fragmentation mechanism was found, in which the ion fragmented upon impact with N_2 (*Phys. Chem. Chem. Phys.,* 2018, **20**, 3614). In using models to interpret experiments of biological ion CID, it is important to know the collision energy threshold for the shattering mechanism. In the work presented here, direct dynamics simulations were performed to study shattering fragmentation versus the collision energy (E_{rel}) for N_2 + $TIK(H^+)_2$. From the probability of shattering fragmentation and the minimum energy transfer for fragmentation versus E_{rel}, a threshold of ~ 55 kcal/mol was identified for N_2 + $TIK(H^+)_2$ shattering fragmentation. This threshold is substantially higher than the lowest activation energy of 14.7 kcal/mol, found from direct dynamics simulations, for the thermal dissociation of $TIK(H^+)_2$.

Collision-induced dissociation (CID) mass spectrometry experiments, in which the fragmenting ion is energized by a single collision at a specified energy, provide the relative abundance of different product ions as a function of energy.[1] These experiments yield important information regarding the primary structure of fragmenting ion and are also particularly useful for understanding the unimolecular kinetics and dynamics of biomolecules, like peptides.[2,3] To interpret these experiments it is important to have a fundamental understanding of the ion's fragmentation dynamics. Once the ion is excited by single-collision CID, the dynamics leading to fragmentation may occur in two limiting ways,[4] analogous to what was identified in surface-induced dissociation (SID) studies.[4-9] The first one is a fully statistical process, in which the translation-to-vibration energy transfer due to the collision between the ion and the inert gas is followed by statistical internal vibrational energy redistribution (IVR) within the energized ion and then the subsequent unimolecular fragmentation dynamics are described by Rice-Ramsperger-Kassel-Marcus (RRKM) theory. The other limiting situation is when the ion fragments during its collision and interaction with the bath gas, in a time which is less than one vibrational period of the fragmenting bond such that there is no IVR. The collision with the bath gas deposits energy in the ion in such a manner that the ion begins fragmenting upon collisional impact. This particular type of non-statistical fragmentation is called "shattering" in SID, and this terminology is retained here for CID. Besides this shattering non-statistical fragmentation, additional non-statistical fragmentation of the ion is expected until IVR is complete. These latter dynamics are referred to as apparent non-RRKM behavior.[10]

In the case of shattering, translation to vibration energy transfer during the collision directly accesses a fragmentation transition state (TS). Previous studies have reported shattering in CID from chemical dynamics simulations and experiments of CH_3SH^+,[11-13] protonated urea,[14,15] and protonated uracil[16,17] and from simulations of $Cr^+(CO)_6$ and $[Li(uracil)]^+$.[18,19] Note that the fragmentation dynamics found from these simulations are in excellent agreement with experiments. Intermediate of these RRKM and shattering limits, a gradation of dynamics is possible; e.g. non-shattering fragmentation, but fragmentation without complete IVR.[20]

An important issue for CID of a peptide ion is the threshold for the shattering mechanism. For example, is shattering important at low collision energies at or near thresholds for peptide ion fragmentation? For the simulations presented here, shattering thresholds are investigated for both backbone and sidechain fragmentations of the doubly protonated tripeptide threonine−

isoleucine−lysine ion, $TIK(H^+)_2$, whose minimum energy structure found from semi-empirical Recife Model 1 (RM1) calculations is shown in Figure 1. In previous simulations,[22] shattering was found to be important for N_2 + $TIK(H^+)_2$ CID at 250, 300 and 690 kcal/mol collision energies. We have thus investigated in more depth details of the threshold energy needed to activate this shattering fragmentation. This system was chosen because it is a relatively extended peptide, with side-chains of different properties, that can be stabilized as doubly-charged species (the second charge being on a side chain) and whose simulation results were discussed with respect to typical peptide and amino-acid fragmentations.[21,22] We have also already studied its statistical fragmentation,[22] such that it is possible to compare the non-statistical shattering and statistical RRKM unimolecular thresholds. Atomistic details of the fragmentation mechanisms were discussed in previous studies[21,22] and here we refer to them. In the work reported here we focus on how shattering evolves as the collision energy is decreased, thus making possible to identify an energy threshold for this particular way of fragmenting. The determination of shattering thresholds is quite important for the use of statistical RRKM modeling to interpret CID experiments of peptide ions.

The simulations reported here were performed with direct dynamics,[23] using the same methodology as described previously for $TIK(H^+)_2$ and $TLK(H^+)_2$ + N_2 collisional direct dynamics,[21] and is only briefly outlined here. A software package consisting of an interface between the VENUS[24,25] classical chemical dynamics and the MOPAC[26] semi-empirical electronic structure theory computer programs was used for the simulations. The RM1 semi-empirical electronic structure theory method[27] was used previously for direct dynamics simulations of $TIK(H^+)_2$ and $TLK(H^+)_2$ fragmentation[21,22] and is also used here. Note that, as from detailed comparison done in our previous work,[21] the fragmentations of $TIK(H^+)_2$ and $TLK(H^+)_2$ are almost identical. Here, for simplicity, we focus on $TIK(H^+)_2$ in order to better discuss the collisional fragmentation and the shattering energy threshold. $TIK(H^+)_2$ was excited about its RM1 global potential energy minimum in Figure 1.[21] Note that RM1 method was shown in the past to correctly describe also gas phase fragmentations of different peptides[28,29] and thus we follow its use also in the present study. Quasi-classical initial conditions[30] were selected for $TIK(H^+)_2$, with its initial vibrational and rotational energies chosen from their 300 K Boltzmann distributions. The initial conditions include the ion's harmonic ZPE. N_2 was in its n = 0 ground vibrational state and its rotational energy was chosen from its 300 K Boltzmann

distribution. Both the ion and N_2 were randomly rotated about their Euler angles. The initial center-of- mass separation between N_2 and $TIK(H^+)_2$ was set at 16.0 Å.

To establish an impact parameter *b* for the current simulations, the distributions of impact parameters leading to shattering for the previous $TIK(H^+)_2$ CID simulations at collision energies of 250 and 300 kcal/mol were investigated. For these simulations *b* was chosen randomly between 0 and 8.5 Å and histograms of the probability of shattering versus *b* are given in Figure 2. With *b* chosen randomly, the probability of a collision with *b* is proportional to *b* and it is seen that the probability of shattering versus *b* is approximately proportional to the probability of a collision versus *b* for a value for *b* up to about 2.5 Å. Following this result, a fixed value for *b* of 2.5 Å was chosen for the simulations reported here to enhance the probability of shattering and to use a value for *b* which is important for collisions.

The N_2 + $TIK(H^+)_2$ simulations were performed for collision energies E_{rel} of 100, 150, 175, 200, and 225 kcal/mol. These energies were chosen in order to slowly decrease from the lowest energy of 250 kcal/mol studied previously[21] to a lower value for which no (or few) shattering trajectories were found. The respective number of trajectories calculated for these energies were 10,338; 7,491; 3,259; 1,928; and 1,237. The total number of trajectories for each value of E_{rel} was chosen in order to have at least about 100 fragmenting trajectories, limiting the maximum number of total trajectories for each set to about 10,000 (this last condition was applied only to the trajectories with the lowest E_{rel} value). Each trajectory was integrated for 2.5 ps. Shattering occurred as N_2 + $TIK(H^+)_2$ collided and interacted. A maximum time for this collisional interaction is 40 fs and fragmentations which occurred within this short time-window were identified as shattering. Similar to the previous simulations of $TIK(H^+)_2$ and $TLK(H^+)_2$ fragmentation,[21,22] a connectivity matrix[21,29] was used to identify reactive trajectories, their fragments, and charges for the fragments.

Four different types of fragmentation mechanisms were observed in the current simulations; i.e. non-shattering fragmentation, backbone and side chain shattering, and shattering forming an H^+ or NH_2^+ ion. In Table 1 we report three percentages which characterize the fragmentation as a function of collision energy (E_{rel}): (i) the percentage of the trajectories which fragmented, (ii) the percentage of shattering trajectories over the number of fragmentation trajectories, and (iii) the percentage of shattering trajectories over the total number of trajectories. There is a substantial decrease in the percentage of the trajectories which

fragmented, with decrease in E_{rel}, ranging from 9.5% at 225 kcal/mol to 0.22% at 100 kcal/mol. Amongst the trajectories which fragmented, the percentage which fragmented by shattering decreased by approximately a factor of 2 with decrease in E_{rel} from 225 to 100 kcal/mol, i.e. from 39.3% to 17.4%. Since the number of shattering trajectories does not depend on the integration time, but the number of fragmenting trajectories does, these percentages depend on the integration time. The percentage which does not depend on integration time is the percentage of shattering trajectories over the total number of trajectories, which is given in Table 1 and also plotted in Figure 3. This percentage decreases from 3.7% at 225 kcal/mol to 0.04% at 100 kcal/mol.

Percentages of the shattering fragmentations which are side chain, backbone, or formation of an H^+ or N_2H^+ ion are given by the bar graph in Figure 4, for collision energies of 150, 175, 200, and 225 kcal/mol. For each energy, the sum of the percentages is 100% and the dominant shattering fragmentation mechanism is formation of an H^+ or N_2H^+ ion. In the case of backbone shattering, they occur primarily from pathways 4 and 6 described in Refs 21 and 22, which correspond to loss of N-terminus and C-terminus groups, forming ions a_1^+ and a_3^{2+}, respectively. The side chain shattering fragmentations correspond mainly to pathway 5 (loss of threonine side chain), pathway 8 (loss of isoleucine side chain), and pathway 9 (loss of terminal part, $CH_2N_3^+$, of lysine side chain), described in the same Refs 21 and 22. At 175, 200, and 225 kcal/mol, the percentages for side chain and backbone shattering are similar. However, at 150 kcal/mol only side chain shattering is observed and its percentage is much smaller than that for H^+ or N_2H^+ formation. The threshold for backbone shattering fragmentation is higher than that for side chain shattering fragmentation or shattering fragmentation forming an H^+ or N_2H^+ ion. While the backbone shattering fragmentations concern parts of the molecule quite exposed to the projectile, the side chains (and also the leaving H^+) are slightly more exposed, being probably the origin of their lower shattering energy threshold.

As shown in Figure 3, the percentage of all the trajectories which are shattering at a specific E_{rel} decreases with decrease in E_{rel}, becoming 0.04% for E_{rel} = 100 kcal/mol. An E_{rel} threshold for shattering will be less than 100 kcal/mol. From the trajectories, it is possible to obtain the amount of collision energy transferred to the ion's internal energy for both shattering and non-shattering trajectories, and for different values of E_{rel}. It results in the distributions of internal energies which are reported in Figure 5. The energy distributions for the non-shattering

trajectories will be a function of simulation time and for the long time limit they will be for statistical fragmentation. For this reason, the minimum internal energies for fragmentation found here for the 2.5 ps "non-shattering" trajectories do not correspond to the statistical limit. This limit was found from a previous statistical study in which the minimum energy threshold was obtained from an Arrhenius plot.[22] On the other hand, shattering trajectories are defined as the ones which fragment in less than 40 fs, and thus they are all inside our simulation time. It is thus possible to identify the minimum transferred energy for which shattering occurs. We should remark that the transferred internal energy is always less than the collision energy (E_{rel}), and it corresponds to the actual activation provided to the ion by the collision. From the energy distributions it is possible to identify the average energy transfers which are listed in Table 2. They are obtained as a function of E_{rel} for all of the fragmentations and then only for the shattering fragmentations. For shattering we report in the same table also the minimum energy transfer, which provides an estimate of the internal energy threshold for shattering. The average energy transfer, for all of the fragmenting trajectories and only the shattering fragmentation trajectories, is statistically the same. In considering all the E_{rel}, the smallest minimum energy transfer for shattering is 55 kcal/mol, which approximates a shattering threshold.

The above threshold is for the b = 2.5 Å simulations reported here and of interest is whether substantially different thresholds are expected for different b. A possible effect of varying b is an increase in rotational energy transfer to TIK$(H^+)_2$ as b is increased. Note that in CID the interaction is repulsive,[31] such that the orbital angular momentum will only add additional repulsion and it does not contribute to a centrifugal barrier which can be important as in ion-molecule reactions where the charge-dipole attractive interaction is important.[32] Since fragmentation results from vibrational energy transfer, an appreciable transfer of the collision energy to rotation would increase the minimum energy transfer for rotation. Information regarding the importance of collision energy transfer to rotation may be obtained from the previous simulations for TIK$(H^+)_2$ and TLK$(H^+)_2$ CID.[22] For these simulations b was chosen randomly between 0 and 9 Å, and the collision energy transferred to rotation is small, 9 kcal/mol as an average corresponding to about 11% of the total transferred energy. This average percentage rotation energy transfer is slightly higher than the 1-3% values found for CID of polyglycines.[33,34] Thus, rotational energy transfer is small for TIK$(H^+)_2$ CID and the current b = 2.5 Å simulations are expected to give a minimum energy transfer threshold for shattering.

In comparison to a shattering threshold of ~ 55 kcal/mol, the lowest threshold found for the thermal dissociation of $TIK(H^+)_2$, with random distribution of its vibrational energy and obtained in the statistical limit from an Arrhenius plot, is 14.7 kcal/mol.[22] Thus, the shattering threshold is significantly higher than that for statistical redistribution of the ion's vibration energy and RRKM unimolecular kinetics. This result shows that shattering does not seem to be important for energies near the fragmentation threshold and thus it would not be important in determining fragmentation products in Threshold-CID experiments.[35,36]

Concluding, for the first time, details of shattering fragmentation are reported for a relatively large peptide ion. An approach is described for obtaining a shattering threshold and applied to a tripeptide, yielding a threshold energy substantially larger than that for statistical RRKM fragmentation. This work may stimulate the determination of shattering and RRKM fragmentation thresholds by comparing collisional simulations at different relative energies with statistical trajectory decompositions done at different temperatures. This approach does not require the location of transition states and, thus, it can be readily applied to complex molecules for which geometrical identification and description of saddle points is often very problematic.

Conflicts of Interest

There are no conflicts to declare.

Acknowledgements

We thank ANR DynBioReact (Grant No. ANR-14-CE06-0029-01), the National Science Foundation under Grant No. CHE-1416428, and the Robert A. Welch Foundation under Grant No. D-0005 for support. The simulations at Texas Tech University were performed with the computer clusters Chemdynm of the Hase Research Group and Hrothgar of the TTU High Performance Computing Center.

References

1. E. de Hoffmann and V. Stroobant. *Mass Spectrometry. Principles and Applications.* John Wiley and Sons, Chichester, 2007.

2. J. S. Brodbelt. *Anal. Chem.,* 2016, **88**, 30.

3. I. A. Papayannopoulos, *Mass Spectrom. Rev.,* 1995, **14**, 49.

4. O. Meroueh and W.L. Hase. *Phys. Chem. Chem. Phys.*, 2001, **3**, 2306.

5. O. Meroueh, Y. Wang and W. L. Hase. *J. Phys. Chem. A*, 2002, **106**, 9983.

6. J. Laskin, T.H. Bailey and J.H. Futrell. *J. Am. Chem. Soc.*, 2003, **125**, 1625.

7. K. Park, B. Deb, K. Song and W.L. Hase. *J. Am. Soc. Mass Spectrom.,* 2009, **20**, 939.

8. S. Pratihar, G.L. Barnes and W.L. Hase. *Chem. Soc. Rev.*, 2016, **45**, 3595.

9. S. Pratihar, G. L. Barnes, J. Laskin and W. L. Hase. *J. Phys. Chem. Lett.*, 2016, **7**, 3142.

10. D.L. Bunker and W.L. Hase. *J. Chem. Phys.* 1978, **59**, 4621-4632.

11. C.-Y. Ng. *J. Phys. Chem. A*, 2002, **106**, 5953.

12. E. Martínez-Núñez, S.A. Vázquez and J.M.C. Marques. *J. Chem. Phys.*, 2004, **121**, 2571.

13. E. Martínez-Núñez, S.A. Vázquez, E.J. Aoiz and J.F. Castillo. *J. Phys. Chem. A*, 2006, **110**, 1225.

14. R. Spezia, J.-Y. Salpin, M.-P. Gaigeot, W.L. Hase and K. Song. *J. Phys. Chem. A*, 2009, **113**, 13853.

15. Y. Jeanvoine, M.-P. Gaigeot, W.L. Hase, K. Song and R. Spezia. *Int. J. Mass Spectrom.*, 2011, **308**, 289.

16. E. Rossich Molina, D. Ortiz, J.-Y. Salpin and R. Spezia. *J. Mass Spectrom.*, 2015, **50**, 1340.

17. E. Rossich Molina, J.-Y. Salpin, R. Spezia and E. Martínez-Núñez. *Phys. Chem. Chem. Phys.*, 2016, **18**, 14980.

18. E. Martínez-Núñez, A. Fernandez-Ramos, S.A. Vázquez, J.M.C. Marques, M. Xue and W.L. Hase. *J. Chem. Phys.*, 2004, **121**, 2571.

19. R. Rodríguez-Fernández, S.A. Vázquez and E. Martínez-Núñez. *Phys. Chem. Chem. Phys.*, 2013, **15**, 7628.

20. W. L. Hase. *J. Phys. Chem.* 1986, **90**, 365.

21. Z. Homayoon, V. Macaluso, A. Martin-Somer, M. C. Nicola-Barbosa-Muniz, I. Borges, Jr., W. L. Hase, and Riccardo Spezia. *Phys. Chem. Chem. Phys.* 2018, **20**, 3614.

22. Z. Homayoon, S. Pratihar, E. Dratz, R. Snider, R. Spezia, G. L. Barnes, V. Macaluso, A. Martin-Somer, and W. L. Hase. *J. Phys. Chem. A,* 2016, **120**, 8211.

23. L. Sun and W. L. Hase. *Rev. Comput. Chem.* 2003, **19**, 79.

24. X. Hu, W. L. Hase and T. Pirraglia. *J. Comput. Chem.,* 1991, **12**, 1014.

25. W. L. Hase, R. J. Duchovic, X. Hu, A. Komornicki, K. F. Lim, D. H. Lu, G. H. Peslherbe, K. N. Swamy, S. R. Vande Linde, A. Varandas, H. Wang and R. J. Wolf. *QCPE Bull.,* 1996, **16**, 671.

26. J. P. Stewart. MOPAC, Colorado Springs, CO, 2012, Stewart Computational Chemistry, HTTP://OpenMOPAC.net.

27. G. B. Rocha, R. O. Freire, A. M. Simas, and J. J.P. Stewart. *J. Comput. Chem.* 2005, **27**, 1101.

28. G. L. Barnes and W. L. Hase. *J. Am. Chem. Soc.* 2009, **131**, 17185-17193.

29. G. L. Barnes, K. Young, L. Yang and W. L. Hase. *J. Chem. Phys.* 2011, **134**, 094106.

30. G. H. Peslherbe, H. Wang, and W. L. Hase. *Adv. Chem. Phys.* 1999, **105**, 171.

31. O. Meroueh and W.L. Hase. *J. Phys. Chem. A* 1999, **103**, 3981-3990.

32. R.D. Levine. *Molecular Reaction Dynamics.* 2005, Cambridge University Press, Cambridge.

33. R.Spezia, J.Martens, J.Oomens, and K.Song. *Int. J. Mass Spectrom.* 2015, **388**, 40.

34. R.Spezia, S.B.Lee, A.Cho, and K.Song. *Int. J. Mass Spectrom.* 2015, **392**, 125.

35. P.B. Armentrout and M.T. Rodgers. *J. Phys. Chem. A* 2000, **104**, 2238-2247.

36. M.T. Rodgers and P.B. Armentrout. *Mass Spectrom. Rev.* 2000, **19**, 215-247.

Table 1. Results from N_2 + TIK$(H^+)_2$ trajectories at different collision energies (E_{rel})

E_{rel} (kcal/mol)	100	150	175	200	225
Number of Trajectories	10338	7491	3259	1928	1237
% Fragmentation	0.22 ± 0.05	1.3 ± 0.1	3.0 ± 0.3	5.7 ± 0.5	9.5 ± 0.8
% Shattering[a]	17 ± 8	29 ± 5	31 ± 5	29 ± 4	39 ± 5
%Shattering[b]	0.04 ± 0.02	0.39 ± 0.07	0.95 ± 0.17	1.7 ± 0.3	3.7 ± 0.5

[a] Percentage of shattering over the number of fragmentation trajectories.

[b] Percentage of shattering over the total number of trajectories.

Table 2. Energy transfer results for reactive trajectories as a function of the collision energy (E_{rel})[a]

E_{rel}	150	175	200	225
Average energy transfer for reactive trajectories	100 ± 15	117 ± 20	139 ± 23	156 ± 25
Average energy transfer when shattering	93 ± 14	111 ± 20	134 ± 29	149 ± 30
Minimum shattering energy transfer	58	55	55	88

[a] Energies in kcal/mol.

Figure Captions

Figure 1. The TIK$(H^+)_2$ minimum energy structure determined from RM1 calculations reported in reference 22.

Figure 2. Number of shattering trajectories versus impact parameter for N_2 + TIK$(H^+)_2$ collisions at E_{rel} of 300 and 250 kcal/mol. The impact parameter is chosen randomly between 0 and 8.5 Å. Results from reference 23.

Figure 3. Percentage of trajectories which are shattering, with respect to the total number of trajectories, versus N_2 + TIH$(H^+)_2$ relative translational energy E_{rel}. The impact parameter is 2.5 Å.

Figure 4. Bar graph of the percentages of the shattering fragmentation which are side chain (blue), backbone (red), and formation of an H-atom or N_2H^+ (green). Total percentage for each energy is 100 %. The impact parameter is 2.5 Å.

Figure 5. Probability of collisional energy transfer to TIK$(H^+)_2$ internal energy for non-shattering and shattering trajectories, with respect to the total number of shattering and non-shattering trajectories. The total probability of each graph is 100 %, with results for different relative translational energies E_{rel}. The impact parameter is 2.5 Å.

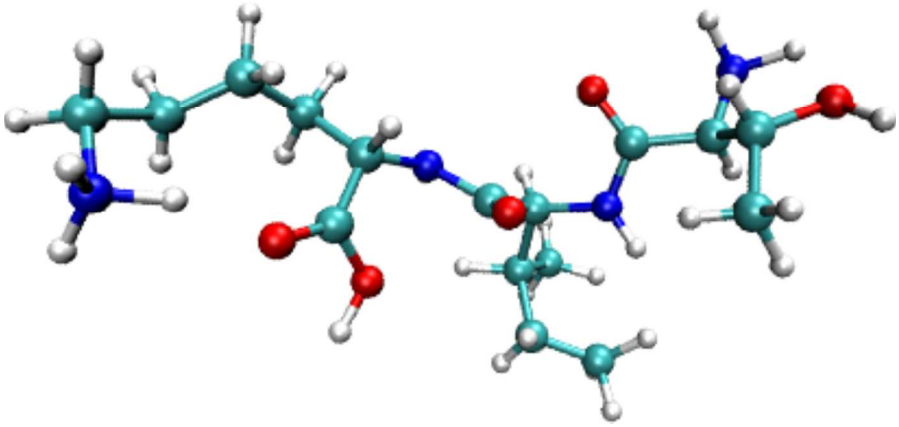

Figure 1

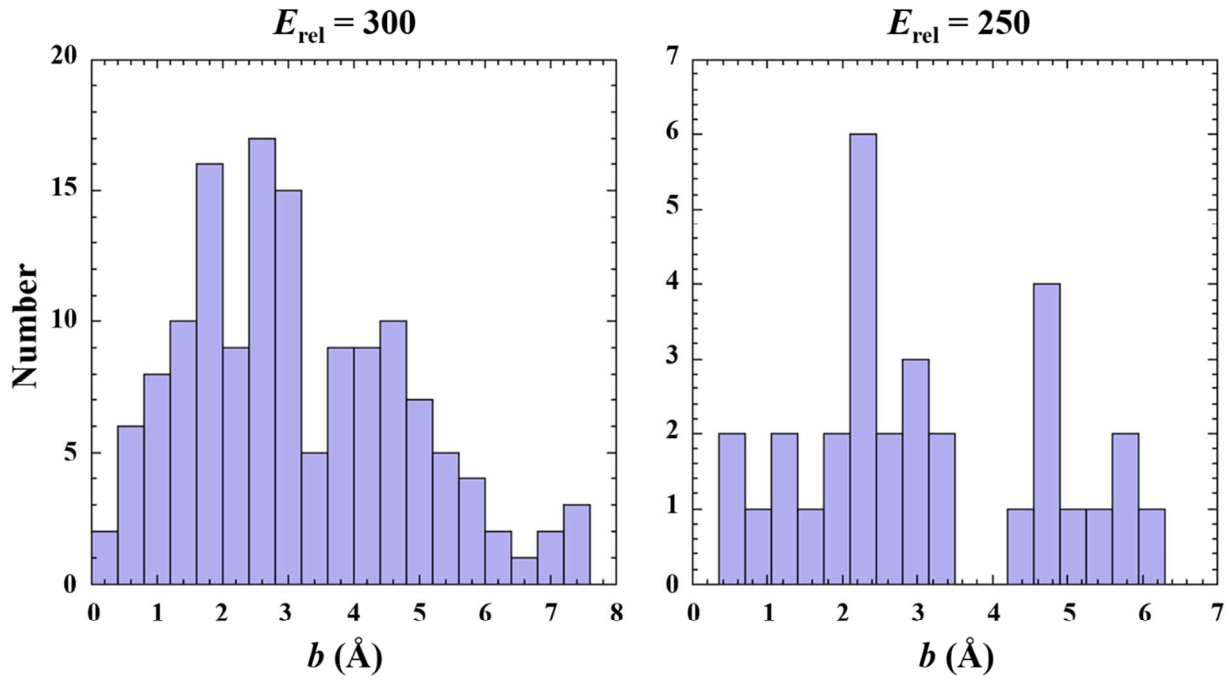

Figure 2

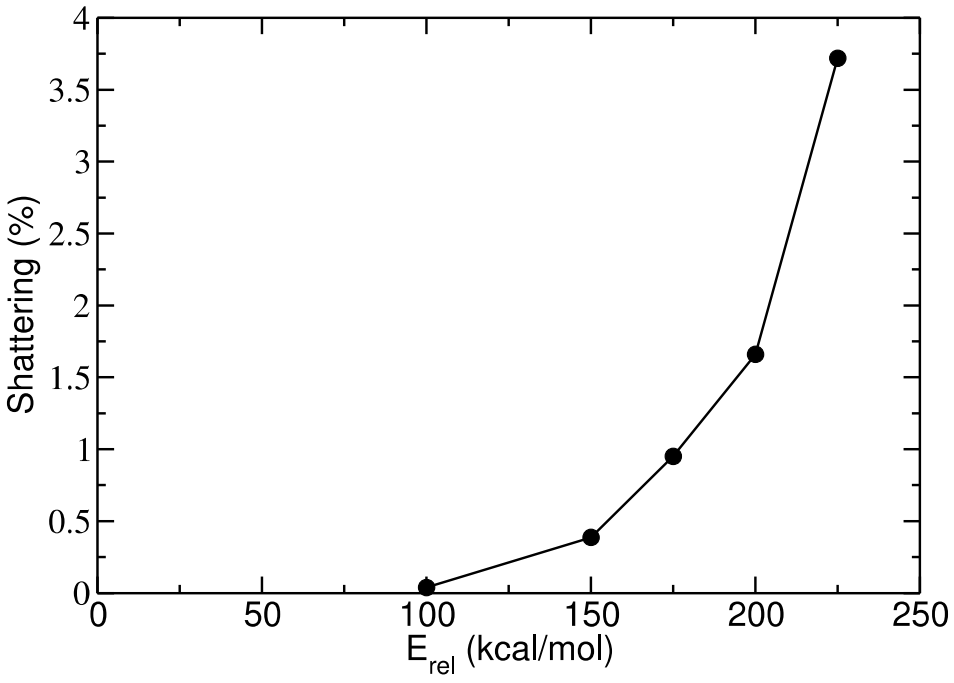

Figure 3

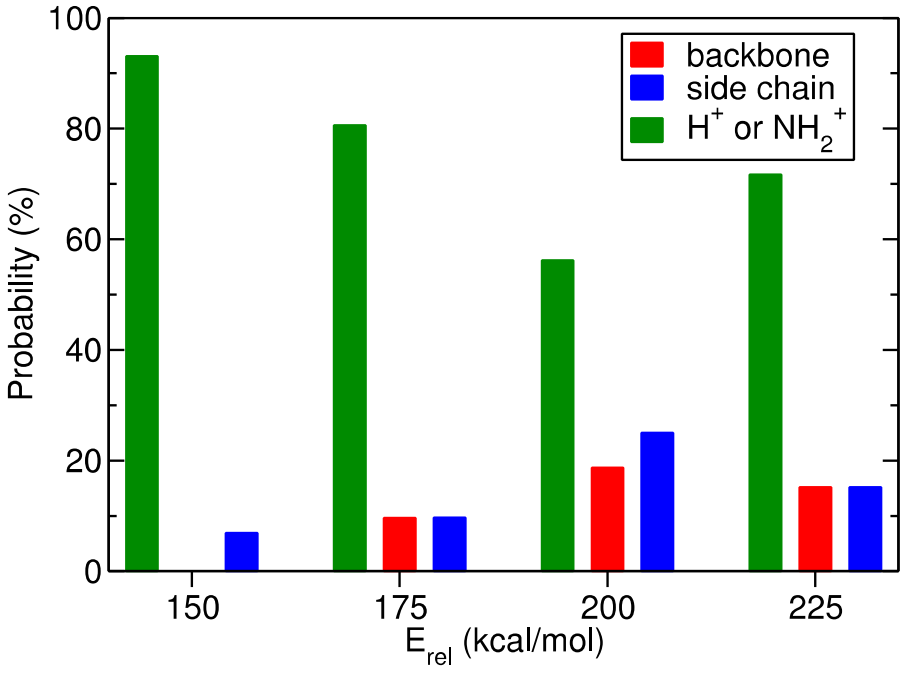
100
80
60
40
20
0
Probability (%)
150
175
200
225
E_rel (kcal/mol)
backbone
side chain
H+ or NH2+

Figure 4

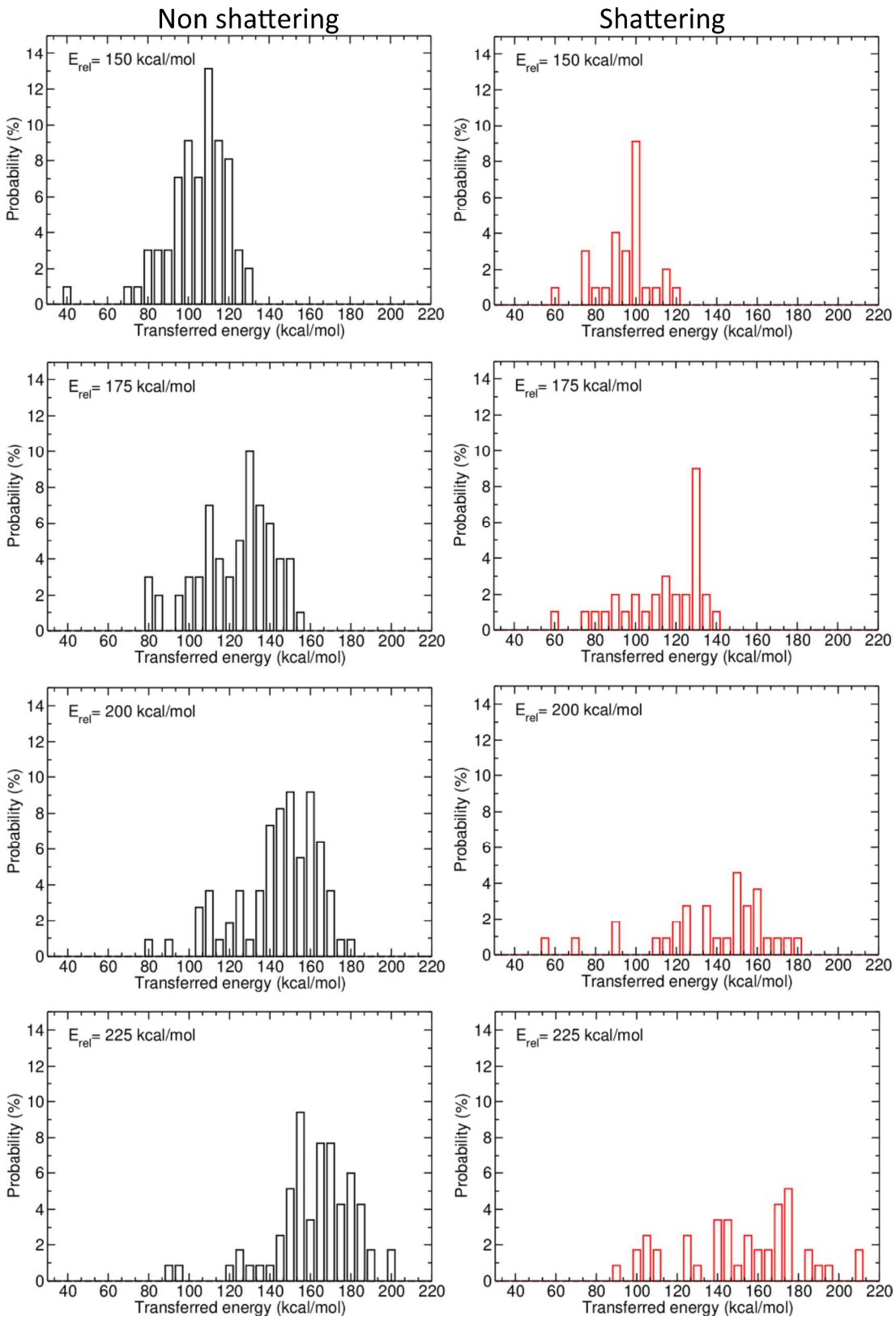
Non shattering
Shattering
E_rel= 150 kcal/mol
E_rel= 175 kcal/mol
E_rel= 200 kcal/mol
E_rel= 225 kcal/mol
Probability (%)
Transferred energy (kcal/mol)

Figure 5

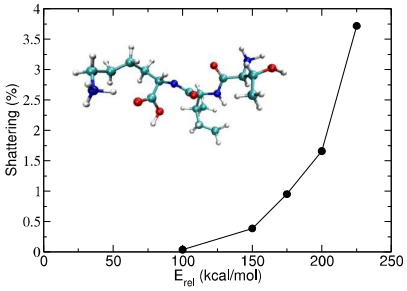

Determination of shattering threshold for unimolecular dissociation of a model tripeptide